Available online at www.sciencedirect.com
SCIENCE DIRECT®
Journal of Organometallic Chemistry 689 (2004) 4783–4790
Journal of Organometallic Chemistry
www.elsevier.com/locate/jorganchem

Bioorganometallic chemistry: biocatalytic oxidation reactions with biomimetic NAD^+/NADH co-factors and $[Cp^*Rh(bpy)H]^+$ for selective organic synthesis

Jochen Lutz [a], Frank Hollmann [a], The Vinh Ho [a], Adrian Schnyder [a], Richard H. Fish [b,*], Andreas Schmid [a,*,1]

[a] *Institute of Biotechnology, Swiss Federal Institute of Technology, ETH Hoenggerberg, HPT, CH-8093 Zurich, Switzerland*
[b] *Lawrence Berkeley National Laboratory, MS-70-108B, University of California, Berkeley, CA 94720, USA*

Received 15 August 2004; accepted 17 September 2004

Abstract

The biocatalytic, regioselective hydroxylation of 2-hydroxybiphenyl to the corresponding catechol was accomplished utilizing the monooxygenase 2-hydroxybiphenyl 3-monooxygenase (HbpA). The necessary natural 1,4-dihydronicotinamde adenine dinucleotide (NADH) co-factor for this biocatalytic process was replaced by a biomimetic co-factor, *N*-benzyl-1,4-dihydronicotinamide, **1b**. The interaction between the flavin (FAD) containing HbpA enzyme and the corresponding biomimetic NADH compound, *N*-benzyl-1,4-dihdronicotinamide, **1b**, for hydride transfer, was shown to readily occur. The in situ recycling of the reduced NADH biomimic **1b** from **1a** was accomplished with [Cp*Rh(bpy)H](Cl); however, productive coupling of this regeneration reaction to the enzymatic hydroxylation reaction was not totally successful, due to a deactivation process concerning the HbpA enzyme peripheral groups; i.e., –SH or $–NH_2$ possibly reacting with the precatalyst, $[Cp^*Rh(bpy)(H_2O)](Cl)_2$, and thus inhibiting the co-factor regeneration process. The deactivation mechanism was studied, and a promising strategy of derivatizing these peripheral –SH or $–NH_2$ groups with a polymer containing epoxide was successful in circumventing the undesired interaction between HbpA and the precatalyst. This latter strategy allowed tandem co-factor regeneration using **1a** or **2a**, $[Cp^*Rh(bpy)(H_2O)](Cl)_2$, and formate ion, in conjunction with the polymer bound, FAD containing HbpA enzyme to provide the catechol product.
© 2004 Elsevier B.V. All rights reserved.

Keywords: Biocatalysis; Co-factor regeneration; Chemoenzymatic reactions; Monoxygenase enzymes; NAD^+/NADH biomimics; Organorhodium hydride; $[Cp^*Rh(bpy)(H)]^+$; Epoxide polymer

1. Introduction

Despite recent advances in catalytic oxyfunctionalization reactions, this class of reactions still represents one of the major challenges for synthetic organic chemistry [1]. The design of efficient catalysts has often been inspired by examples from nature. However, most biomimics do not meet the performances of their natural precedents. In particular, the regio-, chemo-, and enantio-specificity of the catalyzed reactions are not as efficient as the natural enzymes, and include low turnover frequencies (TF), as well as turnover numbers (TN),

* Corresponding authors. Tel.: +1 510 486 4850; fax: +1 510 486 7303 (R.H. Fish), Tel.: +41 1 633 3691; fax: +41 1 633 1051 (A. Schmid).
E-mail addresses: rhfish@lbl.gov (R.H. Fish), andreas.schmid@biotech.biol.ethz.ch, andreas.schmid@bci.uni-dortmund.de (A. Schmid).
[1] Present address: Department of Biochemical and Chemical Engineering, University of Dortmund, Emil Figge Str. 70, D-44227 Dortmund, Germany. Tel.: +49 231 755 7380; fax: +49 231 755 7382.

0022-328X/$ - see front matter © 2004 Elsevier B.V. All rights reserved.
doi:10.1016/j.jorganchem.2004.09.044

which are also several orders of magnitude lower. This above-mentioned situation might also be attributed to the dependency on activated oxygen species, such as peroxides, dioxiranes, or high valent halogen compounds, which are incorporated into the substrate with low selectivity, and frequently at unsatisfactory rates.

Monooxygenase enzymes, on the other hand, utilize molecular oxygen for the specific incorporation of one oxygen into unactivated C–H, C(O)–C, and C=C bonds [2], while minimizing the number of undesired side-reactions. Furthermore, monooxygenase enzymes have been reported to exhibit TF of 10–20 s^{-1} [3], making them highly important catalysts for synthetic organic chemistry purposes. The availability of monooxygenase enzymes, and other aspects associated with preparative scale reactions, as well as stability under process conditions, are now thought to be considered standard practices, while the requirements of reducing equivalents appears to be a continuing challenge [4–6].

In general, monooxygenase enzymes are 1,4-dihydronicotinamde adenine dinucleotide co-factor dependent enzymes; i.e., NADH or NADPH. These co-factors are costly and hydrolytically unstable, and therefore, represent a major barrier for preparative applications utilizing monooxygenases [4,7]. The ribose, pyrophosphate and adenosine groups (Fig. 1) entails the complex structure of NADH, **2b** and NAD(P)H, **3b**, thus making chemical synthesis or isolation from biological sources tedious, and creates the high costs of these biocatalytic processes. It has recently been shown by Lo and Fish [8] that apparently only the nicotinamide ring was required as the redox active site for co-factor regeneration during the enzymatic transfer hydrogenation reaction catalyzed by horse liver alcohol dehydrogenase (HLADH) enzyme, with the finding that *N*-benzylnicotinamide triflate, **1a** (in this paper bromide as the counter ion instead of triflate), and *N*-benzyl-1,4-dihydronicotinamide, **1b**, could be biomimics for natural NAD^+/NADH and provide chiral alcohols from achiral ketones with high enantioselectivity.

To further explore these initial findings on HLADH enzyme recognition of **1b** as an NADH biomimic for reductions of achiral ketones to chiral alcohols, we decided to expand the focus of the NADH model, **1b**,

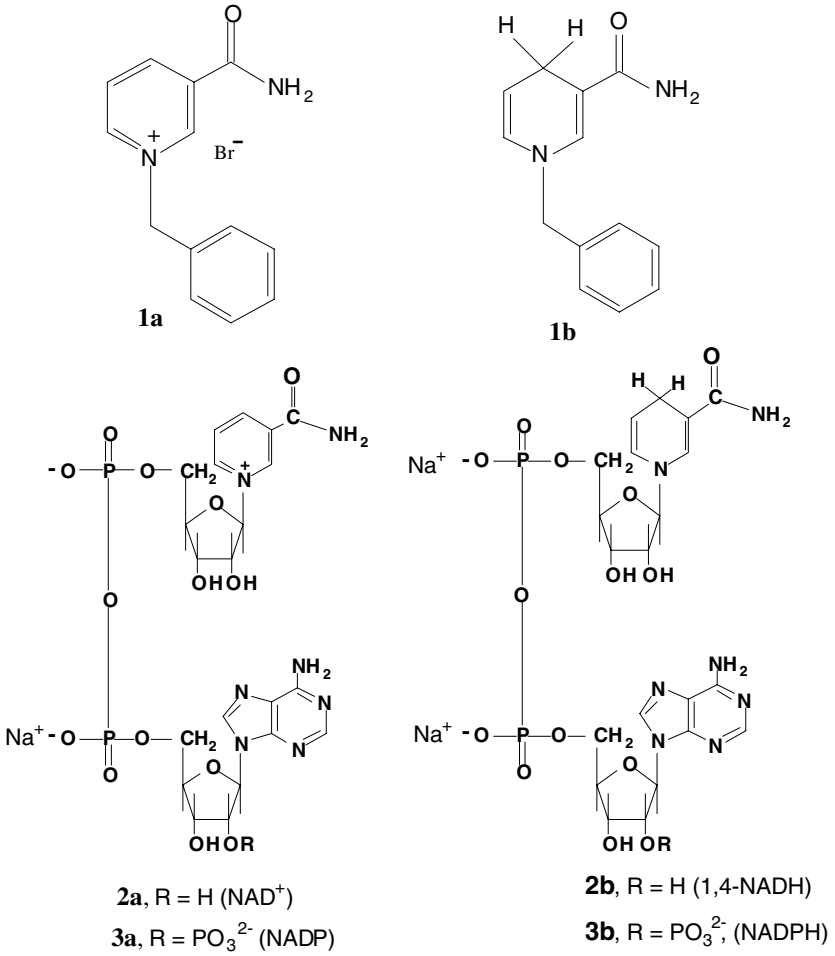

Fig. 1. Structures of *N*-benzylnicotinamide bromide, NAD^+, $NADP^+$ (**1a**, **2a**, **3a**) and *N*-benzyl-1,4-dihydronicotinamide, NADH, NADPH (**1b**, **2b**, **3b**).

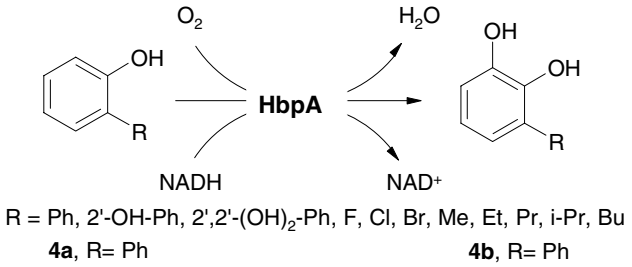

Fig. 2. Enzymatic reaction and substrates that are utilized by 2-hydroxybiphenyl 3-monooxygenase (HbpA).

with a monooxygenase enzyme, 2-hydroxybiphenyl 3-monooxygenase (E.C. 1.14.13.44, HbpA), from *Pseudomonas azelaica* HBP1. The HbpA monooxygenase enzyme catalyzes the specific *ortho*-hydroxylation of a broad range of α-substituted phenols to corresponding catechols (**4b**) (Fig. 2) [9]. The oxidizing species of the enzyme, designated above, is a 4α-hydroperoxo flavin [10]. The latter species was formed in a reaction sequence consisting of hydride transfer from **2b** to the oxidized flavin (FAD), followed by reaction with O_2, and proton abstraction to provide the resulting hydroperoxide. Thus, we will report on the substitution of **2b** by the simple model compound, **1b**, to sustain the catalytic cycle of HbpA. Furthermore, we evaluated the in situ regeneration of **1b** from **1a** using the precatalyst, $[Cp^*Rh(bpy)(H_2O)](Cl)_2$ and sodium formate to catalytically generate, [Cp*Rh(bpy)(H)](Cl), for the regioselective hydrogenation of **1a** to **1b** [14].

2. Results and discussion

Preliminary experiments on the specific *ortho*-hydroxylation of **4a** (2 mM) using HbpA as the enzyme catalyst (substrate/catalyst ratio (S/C): 8300), with 2 mM **1b** as the stoichiometric source of reducing equivalents, resulted in approximately a 6.3% yield of **4b** after 3 h. Thus, the HbpA monooxygenase enzyme performed more than 500 cycles at an average TF of 2.9 min^{-1}. Interestingly, and in contrast to the results of Fish and co-workers [8] with horse liver alcohol dehydrogenase, only a fraction of the potential enzymatic activity of HbpA, (896 min^{-1}), was obtained [11].

To clarify this phenomenon, we further investigated the kinetic properties of HbpA with the reduced nicotinamide model, **1b**. According to the Michaelis–Menten theory, the enzymatic rate is dependent on the binding affinity of HbpA for the substrate **1b**, as well as on the maximum rate for substrate conversion ($v = v_{max} \cdot S/(K_m + S)$). Both parameters ($K_m$, v_{max}) were expected to differ between the natural and the biomimetic co-factor due to the apparent structural differences. Thus, we examined the influence of varying the concentration of **1b** on the conversion rate of **4a** to **4b** (Fig. 3).

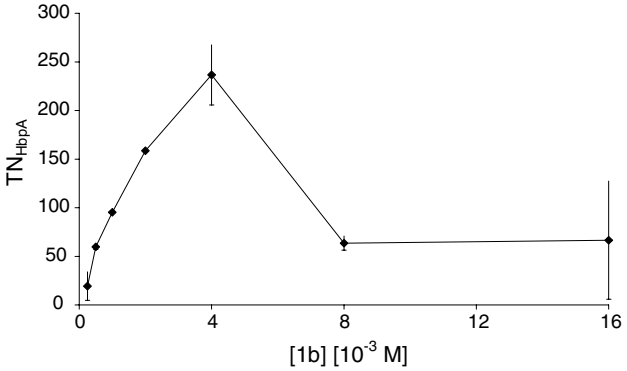

Fig. 3. Dependence of HbpA activity and stability on the concentration of reduced NADH model **1b**. General conditions: 50 mM KP_i-buffer (pH 7.5), $T = 30$ °C; [HbpA] = 0.66×10^{-6} M, [2-hydroxybiphenyl] = 2×10^{-3} M, **4a**, reaction time = 15 min. TN_{HbpA} = turnover number of HbpA (as determined by the amount of product, **4b**, formed).

As shown in Fig. 3, a Michaelis–Menten like activity profile was observed with **1b** concentrations up to 4 mM. Thus, a K_m value of 3.77 mM (0.25 mM $\leqslant$ [**1b**] $\leqslant$ 4 mM) was estimated. This corresponds to an approximately 130-fold decrease in affinity of HbpA towards the NADH model, **1b**, as compared to 27 μM for natural NADH, and readily explains the lower activity observed for HbpA in presence of **1b**. Therefore, at very high concentrations of **1b**, maximum catalytic activity might be expected. Surprisingly, the opposite effect was observed, as further increases of **1b** concentration decreased the initial HbpA activity. Furthermore, we observed that the **1b** oxidation rate was far higher than catechol formation. Similar effects, though to a far lesser extent, had also been observed with **2b** as the reductant, which was explained by the uncoupling of **2b** oxidation from substrate hydroxylation, leading to the formation of hydrogen peroxide [10,11].

Fig. 4 shows a typical reaction profile of the HbpA-catalyzed hydroxylation of **4a** with **1b** as reductant. Less

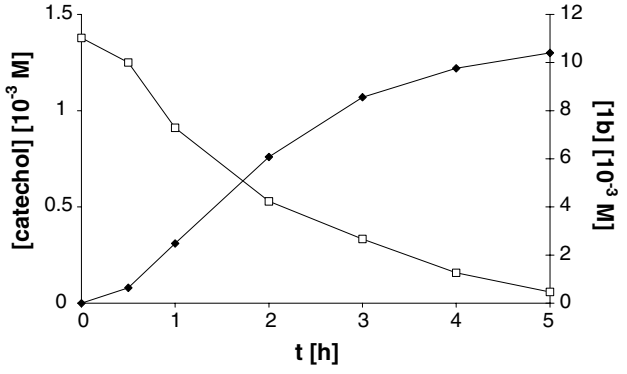

Fig. 4. Reaction profile of a typical enzymatic hydroxylation of 2-hydroxybiphenyl leading to the corresponding catechol (◆), with HbpA promoted by stoichiometric amounts of **1b**, □. General conditions: 50 mM Tris-buffer (pH 7.5), $T = 30$ °C, [HbpA] = 1×10^{-6} M, [2-hydroxybiphenyl] = 2×10^{-3}M.

than 20% of the reducing equivalents provided to HbpA by **1b** were used for productive O_2-activation, i.e., hydroxylation of **4a**. In the case of NADH, **2b**, this value was greater than 85%.

Therefore, we are suggesting that an increased interaction of **1b** with FAD, resulted in hydrogen peroxide formation, rather than in catechol product formation, **4b**. Upon reaction with FAD alone, **1b** was consumed approximately 40 times faster than native NADH, **2b**. Therefore, we concluded that hydride transfer from the reduced pyridine ring to the oxidized FAD alloxazine moiety occurred more efficiently with **1b** than with **2b**.

The dramatically increased rate of **1b** oxidation in comparison to **2b** may be explained by steric, electronic, and conformational effects that facilitate a hydride transfer between **1b** and FAD. Further investigations to clarify this mechanistic point will be accomplished in the future. Based on these results, the interesting dependency of HbpA activity and the concentration of **1b** may be explained by two opposing effects. Firstly, the formation of reduced FAD at the active site was rate limiting in the catalytic mechanism of HbpA. Thus, according to the Michaelis–Menten model, increasing the concentration of **1b** should have increased the rate of the hydroxylation reaction. Moreover, the increased rate of formation of $FADH_2$ also supports the nonproductive generation of hydrogen peroxide (H_2O_2). We suggest that catalytically relevant residues of HbpA, e.g., cysteine SH groups, at the active site of HbpA, were directly affected by in situ generated H_2O_2.

Apparently, the use of **1b** as a reductant does not yield the high correlation between consumption of reducing equivalents and substrate hydroxylation that was observed with natural NADH, **2a** [11]. One plausible approach to rationalising these results assumes that the NADH backbone, presumably via multiple H-bond and other non-covalent interactions, induces major structural changes of the active site geometry, which positions the phenolic substrate in close proximity to the activated 4α-hydroperoxoflavin, thereby minimizing undesired side reactions [12]. Since **1b** lacks the backbone of NADH, none of the aforementioned effects presumably occurs, and the 4α-hydroperoxoflavin becomes susceptible to hydrolysis to H_2O_2 in competition with *ortho* hydroxylation of substrate. Further experiments are currently underway to establish this hypothesis.

We next envisioned in situ regeneration of the biomimetic co-factor, **1b**, using $[Cp^*Rh(bpy)(H_2O)](Cl)_2$ as the precatalyst, with formate as the hydrogen source, to form **1b** from **1a** [14a]. The usual reduction procedure used by enzymologists entails the role of formate dehydrogenase (FDH) to regenerate native NADH, **2b**. However, even after several hours in the presence of 1 mM **1a**, no formation of **1b** was detectable, with FDH as the reducing catalyst. This apparent lack of reactivity of FDH compared to HbpA might be explained by the different enzymatic mechanisms of the FDH reaction for the regeneration of **1b** by formate. For example, Labrou and co-workers described Lys360 to be involved in molecular recognition of **2a** via the ribose ring [13]. FDH brings **2a** and formate in close proximity via specific non-covalent binding of both substrates, which stabilizes the transition state. Thus, the reaction of formate and **2a** was found to be accelerated by several orders of magnitude by FDH. In the case of HbpA, as shown above, the chemical regeneration of $FADH_2$, which is the reactive species for the monooxygenase enzyme, proceeds very rapidly even in the absence of enzyme. Therefore, in the case of **1b**, HbpA was not necessary for the reductive half reaction, i.e., the transfer of hydride to FAD.

The active site of HbpA controls the regiospecific hydroxylation reaction of the substrate via its proximity to the FADH hydroperoxide. Recently, Lo and Fish [8] proposed a possible role for the zinc metal ion center at the active site of HLADH, which was thought to facilitate the stereospecific hydride transfer from **1b** to the achiral ketone substrate for chiral alcohol synthesis. Moreover, in contrast to HLADH, FDH possesses no metal centers to which **1a** might bind, and therefore, be in position in proximity to the formate ion to form **1b**. More importantly, the formate driven regeneration of reduced nicotinamide models, **1a**–**1b** or **2a**–**2b**, has been reported to be catalyzed by the organorhodium hydride, $[Cp^*Rh(bpy)(H)]^+$ [14], with catalytic activities in the range of 11 h^{-1} being observed (Fig. 5).

Thus, we decided to couple the **1b** regeneration as shown in Fig. 5 with the HbpA catalyzed hydroxylation of 2-hydroxybiphenyl. We found only small amounts of product (in the μM range) when combining biomimetic co-factor regeneration with the enzymatic hydroxylation reaction. Further analysis revealed that this lack of catechol product could be explained by the loss of activity of both the organorhodium precatalyst, $[Cp^*Rh(bpy)(H_2O)](Cl)_2$, and the HbpA monooxygenase enzyme under the reaction conditions. Since the general reaction conditions show that each catalytic species was comparatively stable [15,16], we propose an inhibitory interaction between both reactants. In fact, we observed a deactivation of HbpA in the presence of the precatalyst $[Cp^*Rh(bpy)(H_2O)](Cl)_2$, accompanied by the formation of a yellow precipitate (Table 1).

As shown in Table 1, the extent of decreasing HbpA activity depended on both the HbpA and the $[Cp^*Rh(bpy)(H_2O)](Cl)_2$ concentrations, and suggested a stoichiometric interaction of both components causing this inhibition reaction. In a similar situation to the inhibition of HbpA, the $[Cp^*Rh(bpy)(H_2O)](Cl)_2$ activity for the reduction of *N*-benzylnicotinamide bromide, **1a**, in the presence of formate ion, was also decreased. Therefore, we suggest that the potential nucleophilic

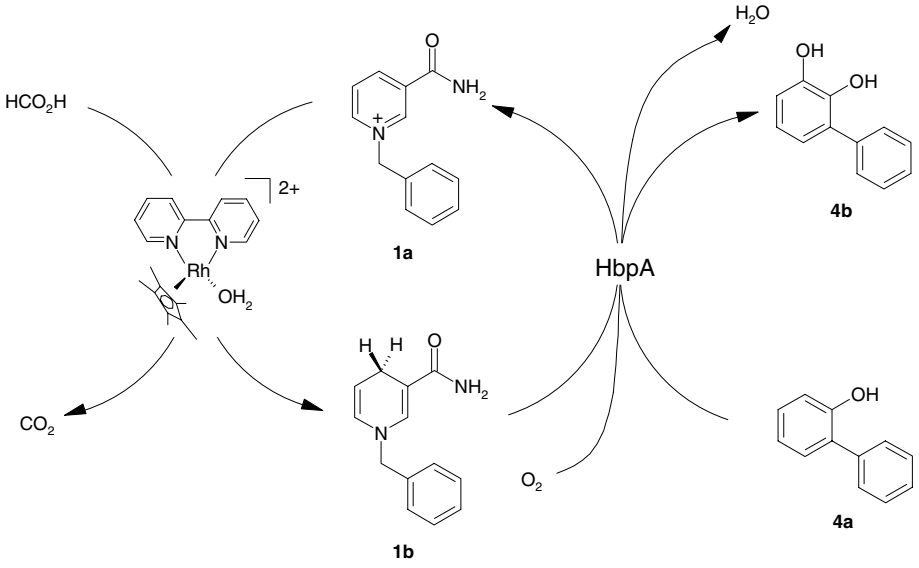

Fig. 5. Tandem co-factor regeneration, using $[Cp^*Rh(bpy)(H_2O)](Cl)_2$ and formate with **1a** (bromide counter ion) to provide **1b**, with a flavin containing and NAD^+ dependent, monooxygenase enzyme, 2-hydroxybiphenyl 3-monooxygenase (HbpA), for selective hydroxylation of 2-hydroxybiphenyl, **4a**, to its catechol derivative, 2,3-dhydroxybiphenyl, **4b**.

Table 1
Deactivation of HbpA and the precatalyst, $[Cp^*Rh(bpy)(H_2O)](Cl)_2$, at different concentrations

c($[Cp^*Rh(bpy)(H_2O)](Cl)_2$) (mM)	c(HbpA) (U ml^{-1})	Residual HbpA-activity (%)[a]
0	0.11	100
0.02	0.11	28
0.04	0.11	8
0.02	0.22	16
	0.44	42
	1.52	68

General conditions: KPi buffer (50 mM, pH 7.5), $T = 30$ °C.
[a] Determined after a 60 min incubation followed by a spectroscopic assay described previously [16].

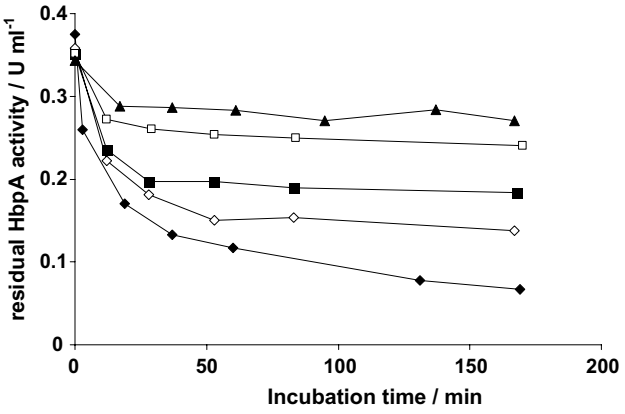

Fig. 6. Influence of various NH_4^+ concentrations on the residual HbpA activity in the presence of $[Cp^*Rh(bpy)(H_2O)](Cl)_2$. General conditions: 50 mM phosphate buffer (pH 7.5, $T = 30$ °C); [HbpA] = 0.39 μM, $[[Cp^*Rh(bpy)(H_2O)](Cl)_2] = 0.04$ mM, [FAD] = 20 μM, $[NH_4^+] = 0$ (▲), 10 (□) 20 (■), 50 (◇), and 100 (◆) mM. At intervals, samples were withdrawn, supplemented with NADH (final 0.2 mM) and 2-hydroxybiphenyl (final 1 mM) and analyzed at $\lambda = 340$ nm.

residues on HbpA, such as lysines ($-NH_2$) or cysteines (–SH), may possibly coordinate to the Cp*Rh metal ion center. A strongly binding amino acid probably will not be displaced by formate ion, therefore, inhibiting the rate of the organorhodium hydride regeneration reaction, and may also explain the deactivation of HbpA. This was demonstrated via the influence of ammonium ions on the HbpA activity in the presence of $[Cp^*Rh(bpy)(H_2O)](Cl)_2$, and is shown in Fig. 6; a clear decrease in activity was noted with increasing ammonium ion concentrations. Therefore, the peripheral groups on HbpA could bind to the $[Cp^*Rh(bpy)(H_2O)](Cl)_2$ dication. via aqua ligand displacement, and possibly affect the ternary structure of HbpA.

Alternatively, we experimented to ascertain if the nucleophilic functional groups on HbpA could be derivatized, and thus prevent the putative $[Cp^*Rh(bpy)(H_2O)](Cl)_2$ deactivation reaction by covalently immobilizing HbpA with Eupergit C, a polymer with epoxide groups that would react with the $-NH_2$ or –SH groups on the HbpA enzyme. Using natural NAD^+, **2a**, as the co-factor, with in situ regeneration catalyzed by $[Cp^*Rh(bpy)H]^+$, resulted in the expected reactivity of HbpA and hydroxylation of **4a** to **4b** with a TF of 4 h^{-1} (Fig. 7); the low TF being a consequence of presumable mass transfer effects associated with the polymer supported enzyme. Furthermore, in similar experiments with **1a**, only trace amounts of **4b** were observed, and we are now conducting experiments to understand the reasons why there was such low product formation.

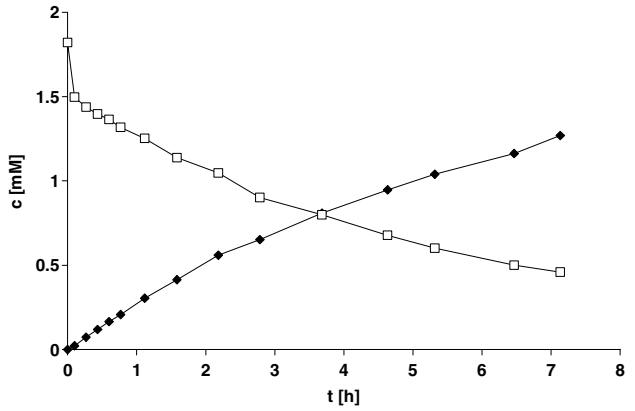

Fig. 7. Chemoenzymatic hydroxylation of 2-hydroxybiphenyl with immobilized HbpA and [Cp*Rh(bpy)(H_2O)]($Cl)_2$ using formate as the source of reducing equivalents, and natural NAD^+, **2a**, as the co-factor. General conditions: potassium phosphate buffer (50 mM, pH 7.5, T = 25 °C), c($NaHCO_2$) = 150 mM, c(HbpA) = 0.175 μM (immobilized on 150 mg Eupergit C), c(NAD^+) = 0.2 mM, c(catalase) = 50 U ml^{-1}, c([Cp*Rh(bpy)(H_2O)]($Cl)_2$) = 0.04 mM (□, 2-hydroxybiphenyl; ◆, 2,3-dihydroxybiphenyl).

3. Conclusions

In the present study, we have extended the use of the biomimetic NAD^+/NADH models, **1a** and **1b**, from previously described horse liver alcohol dehydrogenase to the FAD containing monooxygenase, HbpA [15]. Although the activity of HbpA with the biomimetic NADH co-factor, **1b**, was in the lower percentage range compared to natural NADH, the ease of chemical synthesis of this biomimic, as well as the increased rates of hydride transfer from the reduced biomimetic co-factor, **1b**, directly to FAD provides a simple process for in vitro applications of this and other FAD containing monooxygenases (e.g., styrene monooxygenase, cyclohexanone monooxygenase).

While formate dehydrogenase, FDH, from *Candida boidinii* did not reduce the oxidized biomimic, **1a**, the [Cp*Rh(bpy)(H_2O)]($Cl)_2$/formate system appears to deactivate the HbpA monooxygenase enzyme via binding to functional groups, such as $–NH_2$ and –SH. This deactivation process was somewhat circumvented via derivatization of the enzyme with an epoxide containing polymer to provide, with co-factor **2a**, the hydroxylation product catechol, **4b**, while with biomimic co-factor, **1a**, minor product formation was observed.

In future studies, various strategies will be tested, such as site directed mutagenesis of nucleophilic amino acids, protection of exposed amino acid functional groups by other modifications (acylation, etc.), or directed evolution approaches, to reduce enzyme deactivation by [Cp*Rh(bpy)(H_2O)]($Cl)_2$, while increasing the activity towards the reduced biomimic, **1b**, should also allow satisfactory product formation with other chemoenzymatic cell-free hydroxylation systems.

4. Experimental

4.1. Chemicals and enzymes

All chemicals, benzyl bromide, nicotinamide, sodium dithionite, NADH, FAD, sodium formate, 2-hydroxybiphenyl and 2,3-dihydroxybiphenyl, dioxane, methanol, acetone and buffers, were obtained from Fluka, as well as the enzymes *Candida boidinii* formate dehydrogenase (EC 1.2.1.2) and bovine liver catalase (EC 1.11.1.6) in the highest available quality.

The HbpA (EC 1.14.13.44) was partially purified from recombinant *E. coli* JM101 (pHBP461) [16,17], via anionic expanded bed adsorption chromatography and subsequent desalting, saturation with FAD and dialyzed against 50 mM sodium phosphate buffer of pH 7.5 using a VariPerm L hollow fiber module from Stagroma (Reinach, Switzerland), and stored at −20 °C. The specific activity was calculated to be 0.78 U/mg corresponding to approximately 22% purity. UV activity assays were accomplished as described in the following reference [11].

4.2. Synthesis of *1a*, *1b*, and [Cp*Rh(bpy)(H_2O)]($Cl)_2$

The *N*-benzylnicotinamide bromide (**1a**) was synthesized by dissolving 10 g nicotinamide in 200 ml 1,4-dioxane/50 ml methanol, followed by the addition of 11.6 ml benzyl bromide, and heating for 5 h at 80 °C under reflux. The precipitate was filtered and washed three times with dioxane, recrystallized from methanol, and filtered and dried under vaccum and stored at −20 °C. The bromide anion was not exchanged by precipitaiton with silver triflate (Yield 64% based on nicotinamide), as was described by Fish and coworkers [14a]. The reduced *N*-benzyl-1,4-dihydronicotinamide (**1b**) was obtained by dithionite reduction [18]. Therefore, 2.5 g of **1a**, in presence of 4.6 g sodium carbonate, was dissolved in 60 ml water and reduced by slow addition of sodium dithionite in a 4-fold molar excess for 2 h. The precipitate was filtered, thoroughly washed with water, dried (Yield 82%), stored at −20 °C, and checked by ^1H NMR. The ^1H NMR spectrum of **1b** corresponds to the published spectral data [14a]. The 100 mM stock solutions of **1a** and **1b** in methanol were prepared fresh. The [Cp*Rh(bpy)(H_2O)]($Cl)_2$ complex was synthesized as published elsewhere [5c,14c].

4.3. Biotransformation, co-factor regeneration by [Cp*Rh(bpy)(H_2O)]($Cl)_2$

In typical biotransformations, either 50 mM potassium phosphate or 50 mM Tris buffer of pH 7.5, was used. The 2 mM 2-hydroxybiphenyl (**4a**) (100 mM stock solution in methanol) and typically 2–4 mM **1b** (without in situ co-factor regeneration) or 2–4 mM **1a** in presence

of 10–50 μM $[Cp^*Rh(bpy)(H_2O)](Cl)_2$ and 150 mM sodium formate (with in situ co-factor regeneration) were used at 30 °C and 200–250 rpm. Enzyme concentrations varied from 1/1000 to 1/10 dilutions of an enzyme stock solution of 6.1 U/ml and 7.7 mg/ml protein, but mostly HbpA was diluted 1/15.

4.4. Eupergit immobilisation

The 2 ml HbpA stock solution and 1ml of potassium phosphate buffer (pH 7.5) were incubated at 4 °C for 2 days with 0.4 g Eupergit® C. The immoblisation efficency was calculated from UV enzyme assays [16] and Bradford protein assays [19] of the supernatant, before and after the immobilisation. Immobilisation efficiencies were in the range of 20%. After washing the immobilisates, they were used in biotransformations on a 3 ml scale (see above).

4.5. Analytical techniques

To determine product formation in aqueous solutions, the enzymatic reaction was stopped by the addition of 0.5% (v/v) perchloric acid and the resulting precipitate was removed by centrifugation (20000*g*, 5 min). The samples were analyzed on a LiChroCART® column (125-4 RP-18) using a Merck LaChrom D-7000 high pressure liquid chromatography system (VWR international AG, Switzerland) running under isocratic conditions at 40% acetonitrile and 60% water (0.1% perchloric acid) and 0.75 ml/min flow rate.

4.6. Spectroscopy

The **1b** concentrations were measured at 350 nm, and **2b** concentrations at 340 nm using a Cary 1E (Varian, Switzerland) spectrophotometer. The extinciton coefficient of **1b** was determined to be 5.76 l/(mmol cm)$^{-1}$. Spectra were recorded in quartz cuvettes from 200–600 nm in 15 min intervals.

4.7. Interaction of *1b* or *2b* with FAD

The 0.2 mM FAD, in the presence of either 0.3 mM **1b** or **2b**, were incubated at 30 °C in Tris buffer and the spectra over time were recorded at 15 min intervals. As a control experiment, FAD, **1b**, and **2b** were incubated separately. The time course at 350 nm for **1b** and 340 nm for **2b,** demonstrated the decreases in concentrations of **1b** and **2b** in the presence of FAD.

4.8. Enzymatic regeneration of *1b* by formate dehydrogenase

The 2.5 U formate dehydrogenase was incubated in the presence of 1 mM **1a** and 160 mM sodium formate in 50 mM Tris buffer, pH 7.5 at 30 °C, in a 1 ml cuvette. The UV/Vis spectra were recorded at 15 min intervals. No peak formation at 350 nm (characteristic for **1b**) could be detected during 2 h of incubation, while directly after additon of either 0.5 mM **2a** or 10 μM $[Cp^*Rh(bpy)(H_2O)]^{2+}$ to the above assay, the 350 nm peak was observed.

Acknowledgements

We gratefully acknowledge Martin Neuenschwander for fruitful discussions and for the initial synthesis of *N*-benzyl-1,4-dihydronicotinamide, and Philipp Angerer for support with the ^{1}H NMR experimental measurements. RHF gratefully acknowledges Department of Energy funding to LBNL from the Advanced Energy Projects and Technology Research Division, Office of Computational and Technology Research, under Contract No. DE AC03-76SF00098.

References

[1] (a) E.N. Jacobsen, Acc. Chem. Res 33 (2000) 421;
(b) K.B. Sharpless, Chem. Br. 22 (1986) 38.
[2] (a) V. Ullrich, Angew. Chem., Int. Ed. Engl. 11 (1972) 701;
(b) S. Murai, Activation of Unreactive Bonds and Organic Synthesis, Springer, Verlag, Berlin Heidelberg, 1999;
(c) H.L. Holland, Curr. Opin. Chem. Biol. 3 (1999) 22;
(d) H.L. Holland, H.K. Weber, Curr. Opin. Biotechnol. 11 (2000) 547.
[3] W.A. Duetz, J.B. van Beilen, B. Witholt, Curr. Opin. Biotechnol. 12 (2001) 419.
[4] H.K. Chenault, G.M. Whitesides, App. Biochem. Biotech. 14 (1987) 147.
[5] (a) H.M. Zhao, W.A. van der Donk, Curr. Opin. Biotech. 14 (2003) 583;
(b) M.D. Leonida, Curr. Med. Chem. 8 (2001) 345;
(c) F. Hollmann, P.C. Lin, B. Witholt, A. Schmid, J. Am. Chem. Soc. 125 (2003) 8209;
R. Mertens, L. Greiner, E.C.D. van den Ban, H.B.C.M. Haaker, A. Liese, J. Mol. Catal. B: Enzyme 24-25 (2003) 39;
(d) F. Hollmann, A. Schmid, Biocatal. Biotransform. 22 (2004) 63.
[6] (a) K. Hofstetter, J. Lutz, I. Lang, B. Witholt, A. Schmid, Angew. Chem., Int. Ed. 43 (2004) 2163;
(b) F. Zambianchi, P. Pasta, G. Carrea, S. Colonna, N. Gaggero, J.M. Woodley, Biotechnol. Bioeng. 78 (2002) 488;
(c) U. Schwaneberg, A. Sprauer, C. Schmidt-Dannert, R.D. Schmid, J. Chromatogr. A 848 (1999) 149.
[7] L.J. Rover, J.C.B. Fernandes, G. de Oliveira Neto, L.T. Kubota, E. Katekawa, S.H.P. Serrano, Anal. Biochem. 260 (1998) 50.
[8] H.C. Lo, R.H. Fish, Angew. Chem., Int. Ed. 41 (2002) 478.
[9] A. Schmid, H.-P.E. Kohler, K.-H. Engesser, J. Mol. Catal. B: Enzyme 5 (1998) 311;
M. Held, A. Schmid, H.-P.E. Kohler, W. Suske, B. Witholt, M.G. Wubbolts, Biotech. Bioeng. 62 (1999) 641.
[10] W.A. Suske, W.J.H. van Berkel, H.-P.E. Kohler, J. Biol. Chem. 274 (1999) 33355.
[11] W.A. Suske, M. Held, A. Schmid, T. Fleischmann, M.G. Wubbolts, H.-P.E. Kohler, J. Biol. Chem. 272 (1997) 24257.

[12] (a) A. Meyer, A. Schmid, M. Held, A.H. Westphal, M. Roethlisberger, H.P. Kohler, W.J. van Berkel, B. Witholt, J. Biol. Chem. 277 (2002) 5575;
(b) A. Meyer, Thesis 2002, Swiss Federal Institute of Technology Zurich, Zurich, 2002.
[13] N.E. Labrou, D.J. Rigden, Y.D. Clonis, Eur. J. Biochem. 267 (2000) 6657.
[14] (a) H.C. Lo, O. Buriez, J.B. Kerr, M.M. Olmstead, R.H. Fish, Inorg. Chem. 40 (2001) 6705;
(b) D. Westerhausen, S. Herrmann, W. Hummel, E. Steckhan, Angew. Chem., Int. Ed. Engl. 31 (1992) 1529;
(c) E. Steckhan, S. Herrmann, R. Ruppert, E. Dietz, M. Frede, E. Spika, Organometallics 10 (1991) 1568.
[15] F. Hollmann, B. Witholt, A. Schmid, J. Mol. Catal. B: Enzyme 19–20 (2002) 167.
[16] A. Schmid, I. Vereyken, M. Held, B. Witholt, J. Mol. Catal. B: Enzyme 11 (2001) 455.
[17] J. Lutz, V.V. Mozhaev, Y.L. Khmelnitsky, B. Witholt, A. Schmid, J. Mol. Catal. B: Enzyme 19–20 (2002) 177.
[18] E. Pop, M.E. Brewster, M.J. Huang, N. Bodor, Theochem.-J. Mol. Struc. 102 (1993) 27.
[19] M.M. Bradford, Anal. Biochem. 72 (1976) 248.